DOI: 10.1109/BIOMS.2011.6053684

Fast 3-D Fingertip Reconstruction Using a Single Two-View Structured Light Acquisition

Ruggero Donida Labati, *IEEE, Member*, Angelo Genovese
Vincenzo Piuri, *IEEE, Fellow*, Fabio Scotti, *IEEE, Member*
Department of Information Technology
Università degli Studi di Milano
Milan, 20122, Italy.
{ruggero.donida, angelo.genovese, vincenzo.piuri, fabio.scotti}@unimi.it

***Abstract*—Current contactless fingertip recognition systems based on three-dimensional finger models mostly use multiple views ($N > 2$) or structured light illumination with multiple patterns projected over a period of time. In this paper, we present a novel methodology able to obtain a fast and accurate three-dimensional reconstruction of the fingertip by using a single two-view acquisition and a static projected pattern. The acquisition setup is less constrained than the ones proposed in the literature and requires only that the finger is placed according to the depth of focus of the cameras, and in the overlapping field of views.**

The obtained pairs of images are processed in order to extract the information related to the fingertip and the projected pattern. The projected pattern permits to extract a set of reference points in the two images, which are then matched by using a correlation approach. The information related to a previous calibration of the cameras is then used in order to estimate the finger model, and one input image is wrapped on the resulting three-dimensional model, obtaining a three-dimensional pattern with a limited distortion of the ridges. In order to obtain data that can be treated by traditional algorithms, the obtained three-dimensional models are then unwrapped into bidimensional images.

The quality of the unwrapped images is evaluated by using a software designed for contact-based fingerprint images. The obtained results show that the methodology is feasible and a realistic three-dimensional reconstruction can be achieved with few constraints. These results also show that the fingertip models computed by using our approach can be processed by both specific three-dimensional matching algorithms and traditional matching approaches.

We also compared the results with the ones obtained without using structured light techniques, showing that the use of a projector achieves a faster and more accurate fingertip reconstruction.

***Index Terms*—fingerprint, contactless, three-dimensional, reconstruction, structured light.**

I. Introduction

Today, most of the fingerprint recognition systems use touch-based acquisition sensors. These systems suffer of important problems, such as filth, elastic skin deformations, and the possibility to obtain latent fingerprints from a dirty sensor. At the moment, in fact, one interesting research topic consists in the design of touch-less fingertip recognition systems based on standard CCD cameras. One of the most important problems of touch-less fingertip recognition systems is the lower visibility of the ridge pattern in the captured images. In fact, these images can present reflections, the background is more complex, and the skin itself can be considered as a part of the background. Moreover, the area of the fingertip that can be captured by a single camera is limited and problems related to perspective effects are present.

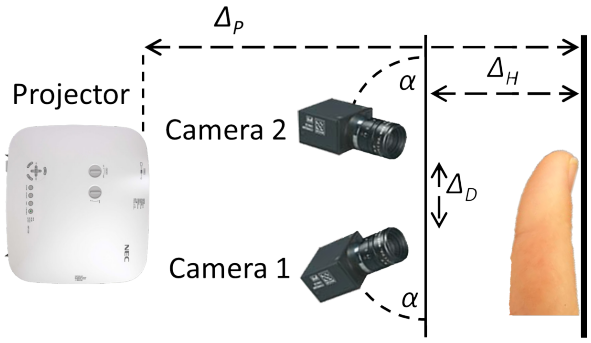

Fig. 1. Schema of the proposed acquisition setup.

Some approaches proposed in the literature consist in image enhancement methods able to render the images captured with a CCD camera compatible with traditional biometric algorithms [1–5]. At the moment, none of these systems reach an accuracy comparable to touch-based systems. Moreover, they do not solve the problems related to perspective effects. One of the most researched possibilities to overcome this problem is the estimation of a three-dimensional model of the fingertip. It would then be possible to reconstruct the ridge pattern without distortions. Some examples of these systems are proposed in [6–8]. Complex and constrained setups are however needed for the three-dimensional reconstruction. They can be based on multiple cameras, special mirrors, and structured light illumination systems. All of them require that the finger is exactly placed and held still during the time needed to perform the biometric acquisitions.

In this paper, we present a novel methodology able to obtain a three-dimensional reconstruction of the fingertip in less constrained conditions than the ones proposed in the literature. The method is based on a single two-view acquisition of the fingertip with the aid of a fixed projected pattern. The

acquisition setup, depicted in Fig. 1, requires only that the finger is placed according to the depth of focus of the cameras, and in the overlapping field of views. Each sample acquisition is done in a single instant of time and no projector calibration is required. The proposed methodology can be applied to a single acquisition composed by two frames, captured using a synchronization trigger. The projected pattern is used in order to extract a set of reference points in the two images, which are rapidly matched by using the geometric information related to the pattern itself. The finger model is then reconstructed by using the information related to a previous calibration of the cameras. A novel algorithm is then used in order to remove the light pattern from the captured images, and one input image is wrapped on the resulting three-dimensional model, obtaining a three-dimensional pattern with a limited distortion of the ridges. Finally, an enhancement method is applied to the texture of the three-dimensional model in order to improve the visibility of the distinctive characteristics of the fingertip. In order to obtain bidimensional data that can be treated by traditional algorithms designed for touch-based fingerprint images, a method for the unwrapping of the three-dimensional models is also proposed.

We also compared our approach with a less expensive variant of the proposed methodology, which does not require the use of a projector, but uses a simple led illumination. The algorithms are very similar to the ones adopted by using the projected pattern. The most important difference consists in the method used for the searching of corresponding pairs of points in the two images.

In this paper, we refer to these approaches as *structured light* and *non-structured light*.

The paper is structured as follows: Section II proposes a literature review, Section III describes the steps of the proposed approach, and Section IV presents the experimental results.

II. Previous Work

The three main categories of contact-less fingertip recognition techniques can be defined as single view systems, multiple view systems and systems based on structured light.

Single view systems are described in [1–3] and propose enhancing algorithms based on the analysis of the frequency and the orientation of the fingertip pattern. The perspective limitation of a single view, however, is an important problem of these systems.

Systems based on multiple views can compute a three-dimensional model of the finger shape or a merged image of the fingertip. A method for the three-dimensional reconstruction of the finger is presented in [6] and uses an illuminator shaped as a ring-mirror. The approach described in [7] is based on a shape from silhouette technique and uses five cameras pointed toward the finger, placed on a support in the middle of the system. The method proposed in [9] does not estimate three-dimensional models but computes the mosaicing of three different views of the finger.

Systems based on structured light compute more accurate three-dimensional models because they are able to estimate also the height of the ridge pattern. These systems, however, require that the finger remains still while the patterns are projected during the biometric acquisition step. The system described in [8,10] is based on the projection of a sinusoidal pattern.

Many of the described approaches deal also with the unwrapping of the three-dimensional model onto a planar surface, in order to perform classical matching techniques on the extracted ridge pattern. An approach described in [11] approximates the three-dimensional model of the finger to a cylinder and transforms the fingertip texture in cylindrical coordinates. A non-parametric approach is also described in [11] and uses local distance measures to preserve the relations between the points of the finger model. The method described in [8] fits multiple circles to the three-dimensional model, using the information related to each circle to perform a geometric mapping. The technique described in [12] is based on the conversion of the three-dimensional points in spherical coordinates, and on a subsequent refinement step. The approach described in [13] computes the fitting plane for each local region of the model and then unwraps the points for each fitted plane, minimizing a cost function which describes the movement exerted between each point and its neighbors.

III. The proposed approach

In this paper we propose an approach able to estimate a three-dimensional model of the finger using only a limited number of reference points, thus achieving a fast reconstruction. The system setup is composed by a pair of CCD color cameras and an off-the-shelf DLP projector which projects a square pattern onto the finger. The pattern is designed in order to be subsequently separated from the fingertip images. The proposed method can be divided in the following steps:

1) camera calibration;
2) pattern projection and acquisition;
3) image preprocessing;
4) extraction and matching of the reference points;
5) three-dimensional surface estimation and image wrapping;
6) texture enhancement;
7) fingertip unwrapping.

In order to evaluate the quality of the obtained results, we used methods designed for touch-based fingerprint images on the images obtained by computing the unwrapping of the estimated three-dimensional models.

The steps of the proposed non-structured light approach are the same of the ones adopted by the structured light approach. The most important difference consists in the extraction and matching of the reference points.

A. Camera calibration

The calibration step is performed off-line once, before the acquisition step, and uses the algorithms described in [14] and [15] in order to compute the intrinsic and extrinsic parameters of the cameras and the stereoscopic setup. The used calibration object is a chessboard, which is captured and

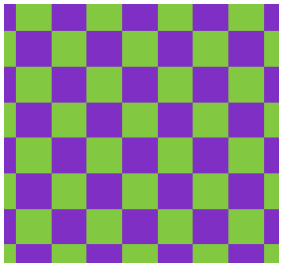

Fig. 2. A portion of the alternate square pattern.

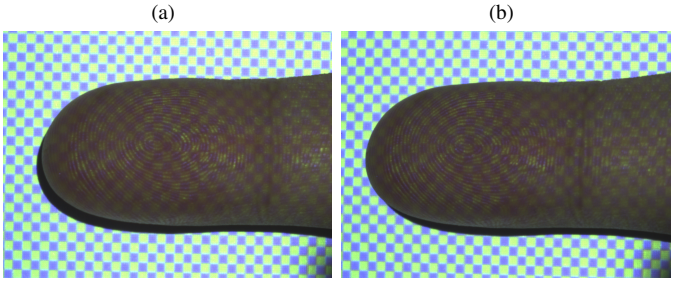

Fig. 3. A two-view acquisition with the structured light pattern.

then processed by using a corner detection algorithm. A DLT method, described in [16], is used to compute the homography matrix.

B. Pattern projection and acquisition

In the literature, some works discuss the possibility to use special projected patterns in order to improve the performance of the stereo matching process [17,18]. However, these systems do not permit to subsequently remove the pattern from the captured image.

In our method, the pattern emitted by the projector is composed by squares with a fixed edge size, with two square colors (green and blue) organized in an alternate fashion. The pattern is computed starting from a RGB image with uniform intensity S and superimposing green and blue squares. In particular, the green squares are obtained by increasing the G channel of a fixed amount Δ_P and decreasing the B channel of the same quantity. Vice-versa, the blue squares are obtained by increasing the B channel and decreasing the G channel by Δ_P:

$$\begin{cases} G_P(x,y) = G(x,y) + \Delta_P \\ B_P(x,y) = B(x,y) - \Delta_P \end{cases} \text{if } (x,y) \in \text{Green square}$$
$$\begin{cases} G_P(x,y) = G(x,y) - \Delta_P \\ B_P(x,y) = B(x,y) + \Delta_P \end{cases} \text{if } (x,y) \in \text{Blue square} \ , \quad (1)$$

where $G(x,y)$ and $B(x,y)$ are the green and blue channels of the grayscale image, $G_P(x,y)$ and $B_P(x,y)$ are the green and blue channels of the resulting alternate square pattern (Fig. 2). The pattern has the particularity that, by summing the G and B channels, it is possible to recover the original image, while performing the subtraction of G and B channels only the square pattern is extracted. The pattern is projected onto the finger using a DLP projector, then a single two-view capture is performed (Fig. 3).

C. Image preprocessing

In our work, we exploit the patter information to obtain a set of tridimensional points on the finger surface, and we recover the finger details of the captured image by reducing the pattern component superimposed on the finger image.

First, the image that describes only the finger details is computed by using the following equation:

$$I_F(x,y) = G(x,y) + B(x,y) \ , \quad (2)$$

where $G(x,y)$ and $B(x,y)$ are the green and blue channels of the captured image and I_F is the resulting grayscale image (Fig. 4a).

This image is then segmented in order to remove both the background and the shadows:

$$I_s(x,y) = \begin{cases} 1 & t_l < I_F(x,y) < t_h \\ 0 & \text{otherwise} \end{cases} \ , \quad (3)$$

where $I_F(x,y)$ is the original image, $I_s(x,y)$ is the binary segmentation mask, t_l and t_h are two experimentally estimated threshold values. In order to assure that no points outside the finger boundary are considered in the point matching step and to reduce possible errors caused by the presence of reflections of the skin, the binary mask is then processed by using a morphological open operation followed by a close operation. These morphological operations are based on a circular structural element with an experimentally estimated value of radius r_s. Since the pixels near to the boundary regions of the finger are often noisy, the region of interest (ROI) of each image is computed by eroding the segmentation mask. The used structural element is a circle with radius r_e.

The square pattern is extracted by:

$$I_{P1}(x,y) = G(x,y) - B(x,y) \ , \quad (4)$$

and then performing a histogram equalization. In order to reduce the presence of noise, a logarithm image is then computed as:

$$I_P(x,y) = \log\left(1 - I_{P1}(x,y)\right). \quad (5)$$

The resulting image I_P is shown in Fig. 4b.

D. Extraction and matching of the reference points

In the literature, several approaches have been proposed in order to extract and match reference points in stereo images. The methods described in [19–21] especially deal with the problem of camera position differences and illumination changes in the left and right image. However, since our setup involves relatively small differences in the camera pose and illumination, our approach proved to be robust using a non-normalized correlation approach.

The image I_P is processed by using a connected component labeling algorithm which extracts the centroids for each square of the projected pattern. The image $1-I_P$ is binarized by using two different threshold values t_w and t_b, obtaining the images

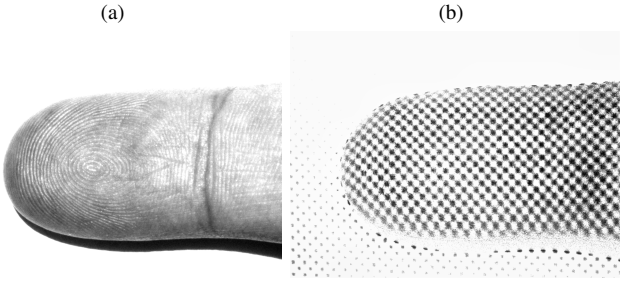

Fig. 4. Separation of finger details and structured light pattern: (a) finger details $I_F(x,y)$ obtained by $G_T(x,y)+B_T(x,y)$; (b) enhanced structured light pattern $I_P(x,y)$ obtained by $G_T(x,y)-B_T(x,y)$, after the histogram stretching and logarithm computation.

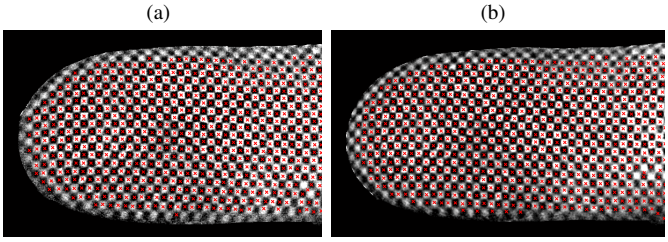

Fig. 5. Extracted reference points: (a) reference points in the first image, (b) reference points in the second image

B_w and B_b. The values of t_w and t_b correspond to 50th and 60th percentile of the histogram related to the image area of I_P that appertains to the ROI. The images B_w and $1-B_b$ are then treated with a morphologic erosion based on a circular structural element with an experimentally estimated value of radius r_c. Finally, the centroids of every 8-connected region are estimated.

The obtained centroids are used as reference points in both the first and the second image (Fig. 5).

In order to minimize the errors due to the incorrect point matching, the matching method is performed twice, first by considering the centroids of the white squares and then considering the centroids of the black squares. The method is based on the information related to the homography matrix computed during the calibration step and on the search of the pairs of points with the highest correlation value: for each reference point $\mathbf{x}_A$ appertaining to the first image I_A, the search for the matching point in the second image is performed by first using the homography matrix to define a preliminary match, according to the formula:

$$\mathbf{X}'_B = H\,\mathbf{X}_A \ , \tag{6}$$

where H is the 3×3 homography matrix, $\mathbf{X}_A$ is the point $\mathbf{x}_A$ expressed in homogeneous coordinates, and $\mathbf{X}'_B$ is the candidate match point in the image I_B expressed in homogeneous coordinates:

$$\mathbf{X}'_B = \begin{bmatrix} X \\ Y \\ W \end{bmatrix} \ . \tag{7}$$

The candidate match point $\mathbf{x}'_B$ in Cartesian coordinates is then computed as follows:

$$\mathbf{x}'_B = \begin{bmatrix} \frac{X}{W} \\ \frac{Y}{W} \end{bmatrix} \ . \tag{8}$$

The correct matching point in the second image is computed by performing the correlation of a $l\times l$ squared window centered in $\mathbf{x}_A$ and the $l\times l$ squared windows centered in the reference points adjacent to $\mathbf{x}'_B$ in the second image (Fig. 6).

The two-dimensional correlation coefficient r is computed according to the formula:

$$r = \frac{\sum_m \sum_n (A_{mn}-\bar{A})(B_{mn}-\bar{B})}{\sqrt{(\sum_m \sum_n (A_{mn}-\bar{A})^2)(\sum_m \sum_n (B_{mn}-\bar{B})^2)}} \ , \quad 1<m<l, \ \ 1<n<l \ , \tag{9}$$

where A and B are the two windows of size $l\times l$. For each reference point $\mathbf{x}_A$ in the first image, the corresponding point in the second image $\mathbf{x}_B$ is chosen as the point with the maximum correlation coefficient. In the case that multiple points in the first image are matched with the same point in the second image, the pair of points with the maximum correlation coefficient value is chosen.

In order to reduce the computational time, we only consider the reference points of the second image with a distance from $\mathbf{x}_A$ on the x and y axes that is less than the empirically estimated values Δ_x and Δ_y respectively.

The non-structured light approach also uses a similar method. This method considers only the information related to the fingertip pattern. The set of reference points is selected by downsampling the image I_A. First, for each reference point $\mathbf{x}_A$, a candidate corresponding point $\mathbf{x}'_B$ is estimated. Then, the matching point $\mathbf{x}_B$ is estimated by searching the point with the highest correlation value r. Differently from the structured light approach, the correlation is not computed by considering $l\times l$ squared windows centered in fixed positions, but the best correlation value is searched by moving the $l\times l$ squared windows for every pixel in a rectangular area with size $w\times h$ centered in the coordinates of $\mathbf{x}'_B$.

E. Three-dimensional surface estimation and image wrapping

A preliminary check for erroneously matched pairs of points is performed by using the Ransac algorithm to fit a homography between the pairs of matched points [22]. The Ransac algorithm discards values which do not fit in the homography estimation, according to a threshold.

A pair of matched points p_i, composed by the points $\mathbf{x}_A$ of the first image and $\mathbf{x}_B$ of the second image, is considered as valid only if:

$$\bar{D}_S - \sigma_{DS} - t_s < d(\mathbf{x}_A,\mathbf{x}_B) < \bar{D}_S + \sigma_{DS} + t_s, \tag{10}$$

where t_s is an empirically estimated value, $d(\mathbf{x}_A,\mathbf{x}_B)$ is the Euclidean distance between the points $\mathbf{x}_A$, $\mathbf{x}_B$, $\bar{D}_S$ and σ_{DS}

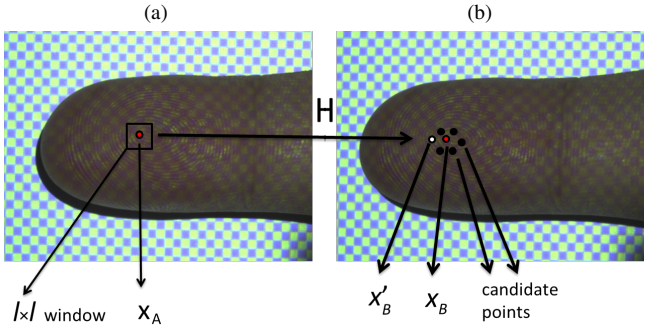

Fig. 6. Matching of the reference points: (a) point x_A in the first image; (b) computation of x'_B and extraction of x_B among the adjacent reference points.

are the weighted mean and the standard deviation of the Euclidean distance related to the nearest n_p pairs of points, with respect to p_i in the first image. The weights used to compute the weighted mean are the inverse of the Euclidean distances between the n_p points nearest to p_i in the first image.

From the matched reference points of the two images and the calibration data, the two-dimensional point coordinates are normalized by using a rectification procedure. The three-dimensional depth coordinate of each point is then computed by using the triangulation formula:

$$z = \frac{fT}{\mathbf{x}_A - \mathbf{x}_B} \tag{11}$$

where f is the focal length of the two cameras, T is the baseline distance between the two cameras and $\mathbf{x}_A$ and $\mathbf{x}_B$ are the two matched points.

For each point $\mathbf{x}_A$, the corresponding three-dimensional coordinates are stored in the vectors X, Y, Z, and the intensity value is stored in the vector C. The last step consists in the computation of the maps M_x, M_y, M_z, M_T, which represent a dense three-dimensional model and the corresponding texture. The maps M_x and M_y are meshed with a constant step s_{interp}, and the maps M_z and M_T are obtained by computing a bilinear interpolation of the estimated vectors Z and C at the coordinates describes by M_x and M_y. Examples of a point cloud and its relative surface estimation are shown in Fig. 7.

F. Texture enhancement

In order to make the contact-less acquisition suitable for traditional minutiae extraction and matching algorithms, we use an enhancing algorithm. This method increases the visibility of the ridges and the contrast of the image, because the fingertip images captured by touch-less sensors often present reflections and a complex background. The proposed method enhances the image by adopting an approach that is similar to the ones proposed in [4,5]. The first step is the enhancement of the ridge visibility and consists in a histogram equalization, background removal, and the computation of the image logarithm. Then, a classical algorithm based on Gabor filters [23] is applied, reducing the noise of the ridge pattern. The last step is an adaptive image binarization.

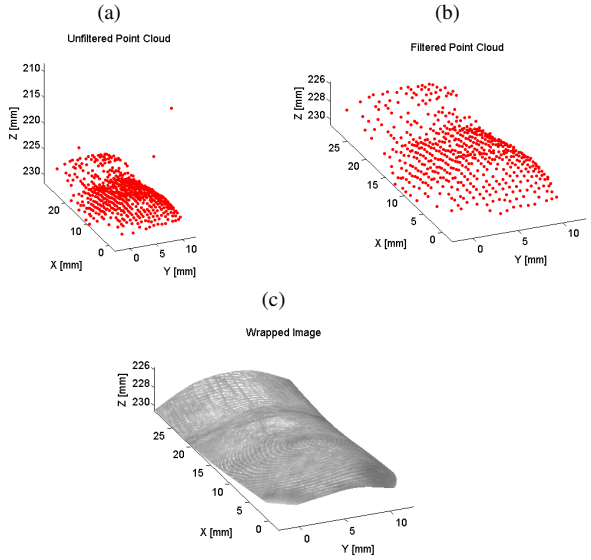

Fig. 7. Three-dimensional point cloud belonging to an index finger before filtering, after filtering and relative texture mapping: (a) unfiltered point cloud; (b) filtered point cloud; (c) texture mapping.

G. Fingertip unwrapping

In order to obtain a bidimensional representation of the biometric sample, which can be processed by classical fingerprint recognition algorithms, an unwrapping method is applied to the three-dimensional models. This method is similar to the algorithm proposed in [8] and approximates the shape of the finger by using rings of different radii.

Starting from the depth map M_z and the matrices M_x, M_y, which describe the three-dimensional model, a circular approximation of the (y, z) values corresponding to each x coordinate of the model is performed by applying the Newton method, obtaining the vectors representing the coordinates (V_{y1}, V_{z1}) of the centers of the circles.

Then, possible outliers are removed by searching the elements of V_{y1} and V_{z1} with a distance greater than the experimentally estimated thresholds t_y, t_z, with respect to the median values of these vectors. The vectors V_{y1}, V_{z1} are then approximated by a first order polynomial, obtaining V_y, V_z.

The vector V_r, which represents the radii of the circles, is then obtained by computing, for each x coordinate of the three-dimensional model, the average distance between the center of the approximating circle $(V_y(x), V_z(x))$ and the coordinates of all the three-dimensional points with said x coordinate, in the matrices M_x, M_y, and M_z. The shape approximation is completed by approximating the vector V_z to a second order polynomial.

The last step consists in the transformation of the fitted model in the bidimensional space. The coordinates of each column x of the matrixes M_y, M_z are transformed in polar coordinates and the corresponding texture values related to the texture map M_T are used to compute the unwrapped image I_U by applying a linear interpolation. A resolution of around 500 ppi is obtained by using an interpolation step of

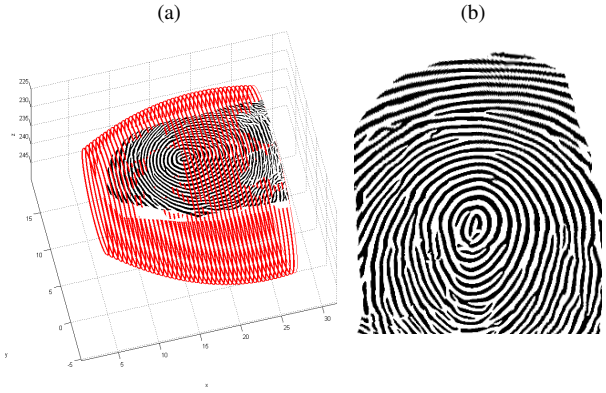

Fig. 8. Using the proposed 3-D samples in classical 2-D applications. Example of three-dimensional unwrapping: (a) fitted three-dimensional model; (b) resulting unwrapped image.

0.0508 mm. Fig. 8 shows an example of the obtained results.

H. Image quality estimation

In order to evaluate the quality of the obtained fingertip images, we use the software NFIQ of the National Institute of Standard and Technology (NIST) [24,25]. This software is based on a neural classifier and returns five different image quality scores. The best image quality corresponds to the score 1, while the worst image quality to the score 5.

IV. Experimental Results

The setup used for capturing the stereo images consists of two Sony XCD-SX90CR CCD color cameras synchronized by using a trigger mechanism. The angle of the cameras with respect to the horizontal support is $\alpha = 85°$, with a baseline distance between the cameras $\Delta_D = 45$ mm (from the centers of the CCDs). The projector is placed with a distance of $\Delta_P = 460$ mm and with an inclination angle $\beta = 15°$ with respect to the surface. The distance from the finger to the cameras is $\Delta_H = 205$ mm. This distance is controlled by using a vertical wooden panel in order to correctly place the finger. The setup is shown Fig. 1. The proposed system can also be mounted vertically and the finger can be placed on a simple desk.

The set of images used for the calibration is composed by 15 pairs of chessboard acquired in different positions. The calibration chessboard is composed by 12×9 squares of 2.8×2.8 mm. We computed from these images a reconstruction error of 0.03 mm of the chessboards in the three-dimensional space. This error is computed by triangulating the two-dimensional coordinates of the chessboard corners, extracted by the calibration algorithm, and computing the interpolating plane of the three-dimensional corner positions. We assumed as an error measure the standard deviation of the Euclidean distance between the triangulated corners and the plane, using an approach similar to the one described in [26].

In the non-structured light configuration, we used a simple led illuminator.

We captured two datasets of images by using the structured light and non-structured light configurations.The two different datasets are obtained by capturing 36 different fingers with the proposed two-view acquisition systems. For each different finger, 10 pairs of images were captured, for a total of 360 pairs of images.

The parameters of the proposed method have been empirically tuned on the used datasets. The value Δ_P used for the computation of the projected pattern is equal to 80; the parameters of the segmentation algorithm are $t_h = 0.9$, $t_l = 0.15$, $r_s = 20$, and $r_p = 40$; the values used by the method for the matching of the reference points are $l = 21$, $\Delta_x = 130$, $\Delta_y = 5$, $w = 130$, and $h = 7$; the parameters used by the three-dimensional estimation algorithm are $t_s = 8$, and $n_p = 8$; the values used by the unwrapping technique are $t_y = 8$, and $t_z = 8$.

The use of the structured light allows to drastically reduce the time needed by the point matching method. In the structured light approach, the search of the matching point in the second image is performed by considering a subset of 60 points adjacent to the candidate point. In the non-structured light approach, we found the minimum size of the search range to contain about 910 pixels. For this reason, the average time needed to reconstruct a three-dimensional point cloud using the projected pattern is decreased by 90%.

We then computed the three-dimensional models by using both the approaches and compared the quality of the resulting unwrapped three-dimensional models. One important quality measure consists in the evaluation of the ridge pattern visibility and distortion after the unwrapping step. In fact, low quality ridge patterns can drastically reduce the accuracy of a biometric recognition system. This analysis is particularly important in the proposed system because an incorrect projected pattern would drastically decrease the visibility of the ridges. Fig. 9 shows two example of enhanced fingertip images after the unwrapping of the three-dimensional models, computed by using the structured linght and non-structured light approaches. It is possible to observe that the use of the structured light does not affect the quality of the resulting textures.

Another important quality measure is the number of outliers that are present in the three-dimensional models. These points, in fact, can produce important distortions of the finger shape, introducing errors in the subsequent unwrapping step. Using the structured light, the number of spikes is much smaller, which allows the use of simpler and faster filtering techniques and also results in a more accurate three-dimensional reconstruction. Fig. 10 shows a comparison with both the filtered and unfiltered point clouds and the respective surface estimations. It is possible to observe that, with the aid of the structured light, the small number of outliers does not affect the surface estimation and they can be easily removed.

In order to numerically evaluate the quality of the reconstructed models, we tested the unwrapped images related to each reconstructed fingertip model by using the NIST NFIQ software. The quality of the unwrapped images, in fact, is strictly related to the presence of spikes and to the correctness of the ridge pattern. The obtained results are summarized in Table I.

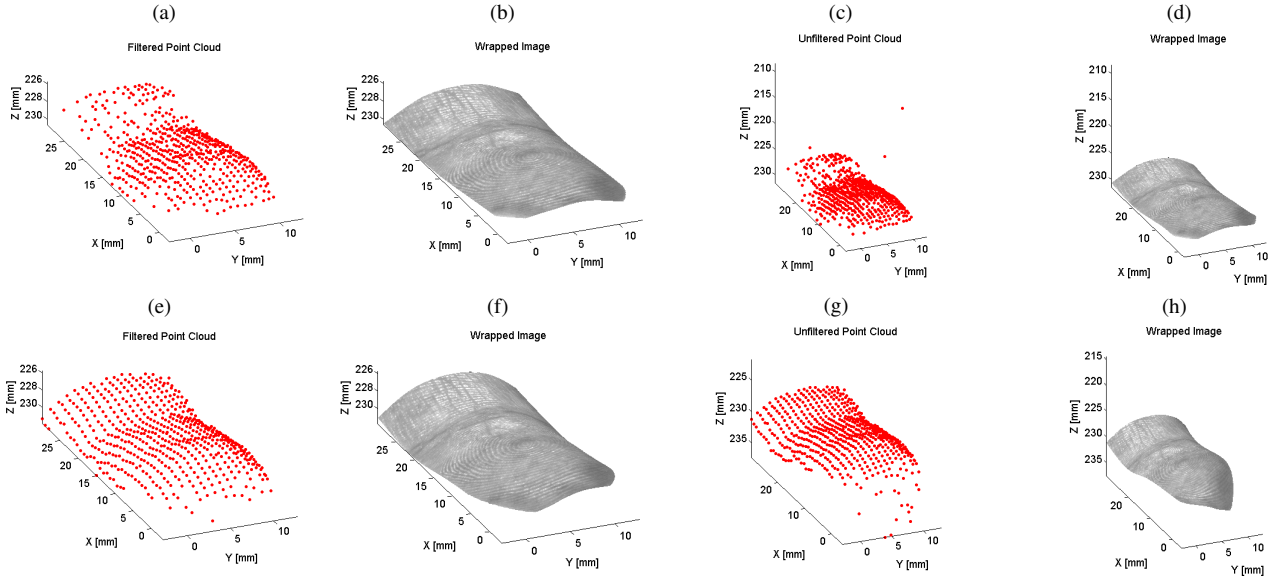

Fig. 10. Three-dimensional point clouds, filtered and unfiltered, computed with the structured light and non-structured light approaches: (a,b): filtered point cloud and surface mapping using the structured light approach; (c,d): unfiltered point cloud and surface mapping using the structured light approach; (e,f): filtered point cloud and surface mapping using the non-structured light approach; (g,h): unfiltered point cloud and surface mapping using the non-structured light approach.

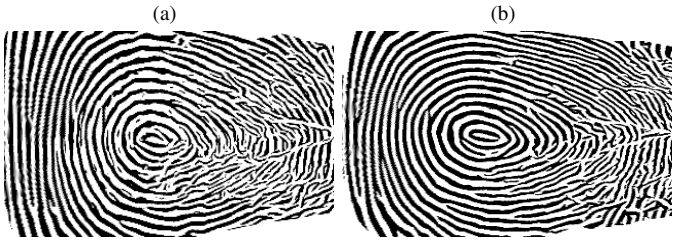

Fig. 9. Enhanced images obtained by unwrapping the three dimensional models computed by using the structured light and non-structured light approaches: (a) image obtained by using the structured light approach; (b) image obtained by using the non-structured light approach. The usage of the structured light can speed-up the creation of the 3D templates up to 90%.

TABLE I
NUMERICAL EVALUATION OF THE OBTAINED FINGERTIP TEXTURES AFTER THE UNWRAPPING STEP.

Structured light		**Non-structured light**	
Mean	**Std**	**Mean**	**Std**
1.380	0.840	1.890	1.120

Table I shows that the quality of the unwrapped images is better for the fingertip models obtained using the structured light approach. This result is related to the fact that the presence of spikes influences the quality of the images obtained by the used fingertip unwrapping method.

V. CONCLUSIONS

The paper presented a novel methodology which combines a 2-view system with the use of structured light for a single biometric acquisition. The method computes a three-dimensional model of the finger and is less constrained than the ones presented in the literature, with both less spatial constraints and time constraints. The system, in fact, requires only that the finger is placed in the depth-of-focus of the cameras and in the overlapping area of their respective field-of-views, without the need of a projector calibration. The acquisition, moreover, is composed by a single two-view synchronized capture.

The method exploits a novel algorithm able to separate the superimposed pattern from the finger details. It uses the projected pattern to obtain a set of reference points used to fast compute the three-dimensional model of the fingertip. The model is then completed with the fusion of the original images, in order to minimize the perspective distortion introduced by the acquisition. A texture enhancing step is performed and then the three-dimensional model is unwrapped by using a multiple circle fitting method.

The quality of the fingertip images obtained after the unwrapping step was compared with the results obtained by the same method performed without the use of the structured light (uniform illumination) by using well-known software designed for touch-based fingerprint images. The results of the fingertip quality analysis applied on the unwrapped fingertip images showed that the proposed method can be used to obtain good-quality fingertip images, suitable to be processed by using classical matching algorithms. Results show that the method is feasible and can achieve an accurate three-dimensional reconstruction. The use of the structured light achieves a major improvement in terms of speed (90%), allowing a real-time reconstruction.

REFERENCES

[1] Y. Song, C. Lee, and J. Kim, "A new scheme for touchless fingerprint recognition system," *2004 International Symposium on Intelligent Signal Processing and Communication Systems (ISPACS 2004)*, pp. 524–527, November 2004.

[2] B. Hiew, A. Teoh, and Y. Pang, "Touch-less fingerprint recognition system," *IEEE Workshop on Automatic Identification Advanced Technologies*, pp. 24–29, June 2007.

[3] V. Piuri and F. Scotti, "Fingerprint biometrics via low-cost sensors and webcams," *2nd IEEE International Conference on Biometrics: Theory, Applications and Systems (BTAS 2008)*, pp. 1–6, October 2008.

[4] R. D. Labati, V. Piuri, and F. Scotti, "A neural-based minutiae pair identification method for touchless fingeprint images," in *IEEE Symposium Series in Computational Intelligence 2011 (SSCI 2011)*, April 2011.

[5] ——, "Measurement of the principal singular point in fingerprint images: a neural approach," in *2010 IEEE International Conference on Computational Intelligence for Measurement Systems and Applications (CIMSA)*, September 2010, pp. 18–23, 978-1-4244-7228-4.

[6] G. Parziale, "Touchless fingerprinting technology," *Advances in Biometrics*, pp. 39–62, 2007.

[7] G. Parziale, E. Diaz-Santana, and R. Hauke, "The Surround Imager^{TM}: A multi-camera touchless device to acquire 3d rolled-equivalent fingerprints," *Lecture Notes in Computer Science*, vol. 3832, pp. 244–250, 2005.

[8] Y. Wang, L. G. Hassebrook, and D. L. Lau, "Data acquisition and processing of 3-D fingerprints," *IEEE Transactions on Information Forensics and Security*, vol. 5, no. 4, pp. 750–760, December 2010.

[9] H. Choi, K. Choi, and J. Kim, "Mosaicing touchless and mirror-reflected fingerprint images," *IEEE Transactions on Information Forensics and Security*, vol. 5, no. 1, pp. 52–61, March 2010.

[10] Y. Wang, L. G. Hassebrook, and D. L. Lau, "Noncontact, depth-detailed 3D fingerprinting," *SPIE Newsroom*, November 2009.

[11] Y. Chen, G. Parziale, E. Diaz-Santana, and A. Jain, "3D touchless fingerprints: Compatibility with legacy rolled images," *2006 Biometrics Symposium*, 2006.

[12] Y. Wang, L. G. Hassebrook, and D. L. Lau, "Fit-sphere unwrapping and performance analysis of 3D fingerprints," *Applied Optics*, vol. 49, no. 4, pp. 592–600, 2010.

[13] L. G. H. Sara Shafaei, Tamer Inanc, "A new approach to unwrap a 3-D fingerprint to a 2-D rolled equivalent fingerprint," *IEEE 3rd International Conference on Biometrics: Theory, Applications, and Systems, 2009. (BTAS'09)*, pp. 1–5, September 2009.

[14] Z. Zhang, "A flexible new technique for camera calibration," *IEEE Transactions on Pattern Analysis and Machine Intelligence*, vol. 22, no. 11, pp. 1330–1334, 2000.

[15] J. Heikkila and O. Silvén, "A four-step camera calibration procedure with implicit image correction," *IEEE Computer Society Conference on Computer Vision and Pattern Recognition (CVPR'97)*, pp. 1106–1112, 1997.

[16] R. I. Hartley and A. Zisserman, *Multiple View Geometry in Computer Vision*, 2nd ed. Cambridge University Press, ISBN: 0521540518, 2004.

[17] J. Lim, "Optimized projection pattern supplementing stereo systems," in *Robotics and Automation, 2009. ICRA '09. IEEE International Conference on*, may 2009, pp. 2823–2829.

[18] J. Pagès, J. Salvi, C. Collewet, and J. Forest, "Optimised De Bruijn patterns for one-shot shape acquisition," *Image and Vision Computing*, vol. 23, pp. 707–720, 2005.

[19] Y. S. Heo, K. M. Lee, and S. U. Lee, "Robust stereo matching using adaptive normalized cross-correlation," *Pattern Analysis and Machine Intelligence, IEEE Transactions on*, vol. 33, no. 4, pp. 807–822, april 2011.

[20] A. Donate, X. Liu, and E. Collins, "Efficient path-based stereo matching with subpixel accuracy," *Systems, Man, and Cybernetics, Part B: Cybernetics, IEEE Transactions on*, vol. 41, no. 1, pp. 183–195, feb. 2011.

[21] W. Li, H. Yao, R. Ji, P. Xu, X. Liu, and D. Zhao, "Robust stereo matching combining sift descriptor with ncc under mrf framework," in *Pervasive Computing Signal Processing and Applications (PCSPA), 2010 First International Conference on*, sept. 2010, pp. 1018–1021.

[22] P. D. Kovesi, "MATLAB and Octave functions for computer vision and image processing," Centre for Exploration Targeting, School of Earth and Environment, The University of Western Australia, available from: <http://www.csse.uwa.edu.au/∼pk/research/matlabfns/>.

[23] L. Hong, Y. Wan, and A. Jain, "Fingerprint image enhancement: Algorithm and performance evaluation," *IEEE Transactions on Pattern Analysis and Machine Intelligence*, vol. 20, pp. 777–789, 1998.

[24] C. I. Watson, M. D. Garris, E. Tabassi, C. L. Wilson, R. M. McCabe, S. Janet, and K. Ko, "User's guide to nist biometric image software (NBIS)," National Institute of Standards and Technology, January 2007, http://fingerprint.nist.gov/NFIS.

[25] M. Garris, E. Tabassi, and C. Wilson, "Nist fingerprint evaluations and developments," *PIEEE*, vol. 94, no. 11, pp. 1915–1926, November 2006.

[26] R. Guerchouche and F. Coldefy, "Camera calibration methods evaluation procedure for images rectification and 3D reconstruction," *Orange Labs, France Telecom R & D*, 2008.